THE JOURNAL OF BIOLOGICAL CHEMISTRY VOL. 281, NO. 34, pp. 24769–24780, August 25, 2006

Serotonin-, Protein Kinase C-, and Hic-5-associated Redistribution of the Platelet Serotonin Transporter*

Received for publication, April 24, 2006, and in revised form, June 19, 2006 Published, JBC Papers in Press, June 27, 2006, DOI 10.1074/jbc.M603877200

Ana Marin D. Carneiro[‡] **and Randy D. Blakely**[‡§1]

From the Departments of [‡]*Pharmacology and* [§]*Psychiatry, Center for Molecular Neuroscience, Vanderbilt University School of Medicine, Nashville, Tennessee 37232-8548*

Emerging data indicate the existence of multiple regulatory processes supporting serotonin (5HT) transporter (SERT) capacity including regulated trafficking and catalytic activation, influenced by post-translational modifications and transporter-associated proteins. In the present study, using differential extraction and sedimentation procedures optimized for the purification of cytoskeletal and membrane-skeletal associated proteins, we analyze SERT localization in platelets. We find that most of the plasma membrane SERT is associated with the membrane skeleton. This association can be enhanced by both transporter activation and 5HT2A receptor activation. Inactivation of transport activity by phorbol ester treatment of intact platelets relocates SERT to the cytoskeleton fraction, consequently leading to transporter internalization. The translocation of SERT between these compartments is correlated with changes in the interaction with the LIM domain adaptor protein Hic-5. Co-immunoprecipitation and uptake activity studies suggest that Hic-5 is a determinant of transporter inactivation and relocation to a compartment subserving endocytic regulation. Associations of SERT with Hic-5 are evident in brain synaptosomes, suggesting the existence of parallel mechanisms operating to regulate SERT at serotonergic synapses.

Serotonin (5-hydroxytryptamine, 5HT)[2] is an important mediator of cell-to-cell signaling in both neuronal and non-neuronal systems. Following release, the extracellular levels of 5HT are controlled by the antidepressant-sensitive 5HT transporter (SERT, 5HTT), a member of the Na^+/Cl^--dependent transporter family (SLC6) (1). Alterations in SERT-mediated 5HT clearance have a significant effect on serotonergic signaling and behavior, demonstrated by both pharmacological and genetic studies (2–4). 5HT-selective reuptake inhibitors (SSRIs) target SERT and are widely used to treat multiple psychiatric syndromes including depression, panic disorder, obsessive-compulsive disorder (OCD), and autism (5–7). SERTs are also targets of multiple psychostimulants (*e.g.* cocaine, MDMA "ecstasy") and thus likely also play a critical role in the mechanisms of substance abuse (8–10). In neurons, SERT is predominantly localized in axon terminal membranes and present in low levels at the cell body and dendrites, suggesting that SERT function is dependent upon its subcellular localization (11, 12). The mechanisms that specify the plasma membrane localization of SERT are as yet ill defined.

The plasma membrane is organized in specialized domains anchored to actin filaments that include spectrin-based meshworks, adsorptive cell surface microvilli, focal adhesions, and adherens junctions (13, 14). In each of these domains, interactions between cytoskeletal proteins provide resistance against disruption by nonionic detergents, such as Triton X-100, permitting the transmembrane protein assembly to be isolated as a "membrane skeleton" (15, 16). Fox *et al.* (17, 18) have suggested the membrane skeleton as a platform for mediating signal transduction. Of particular interest is the involvement of the membrane skeletal elements in mediating or inhibiting movements of cell surface receptors, and their participation in the formation of specialized domains and in signal transduction at the plasma membrane (19–21). Lipid-lipid interactions also can organize membranes into detergent-resistant domains, morphologically denominated caveolae (22). Such lipid "rafts" are stabilized against disruption by cold Triton X-100 through liquid-ordered packing of component cholesterol, sphingolipids and glycerolipids (23). Lipid rafts also have been proposed to play roles in membrane targeting and endocytotic trafficking (24, 25).

Both cytoskeleton-stabilized membrane domains and lipid rafts provide sites at which localized signal transduction that ultimately modulate SERT function could occur. Cholesterol depletion of HEK-293 cells expressing rSERT modifies both ligand and antidepressant-binding affinities to the transporter through a mechanism that may involve direct cholesterol/transporter interactions (26). Whereas active SERT expressed in HEK-293 cells has been localized to lipid rafts, phorbol ester treatment of synaptosomes relocates SERT away from lipid raft fractions in concert with a loss of associated proteins (27). SERTs form complexes with a growing list of membrane proteins, enzymes and cytoskeleton-associated proteins including syntaxin 1A (28, 29), PP2Ac (30), MacMARCKS (31), and Hic-5 (32), although the precise role of these associations is not fully defined. Additional information regarding SERT subcellular localization in the context of regulated protein associations may provide important clues to precise mechanisms of SERT regulation.

* This work was supported by National Institutes of Health Grants T32 MH65782 and T32 MH65215 (to A. M. D. C.) and DA07390 (to R. D. B.). The costs of publication of this article were defrayed in part by the payment of page charges. This article must therefore be hereby marked "*advertisement*" in accordance with 18 U.S.C. Section 1734 solely to indicate this fact.

[1] To whom correspondence should be addressed: 7140 MRBIII, Vanderbilt School of Medicine, Nashville, TN 37232-8548. Tel.: 615-936-3705; Fax: 615-936-3040; E-mail: randy.blakely@vanderbilt.edu.

[2] The abbreviations used are: 5HT, serotonin; PBS, phosphate-buffered saline; PKC, protein kinase C; SERT, serotonin transporter; MAPK, mitogen-activated protein kinase; Ab, antibody; MS, membrane skeleton; TS, Triton soluble; CS, cytoskeletal pellets; PMA, phorbol 12-myristate 13-acetate.

Specific binding to a particular membrane skeleton/cytoskeleton may also be controlled by phosphorylation (17). SERT exhibits basal phosphorylation that can be elevated by activation of protein kinases and inhibition of protein phosphatase 2A, with accompanied changes in transport activity and/or surface expression (33). External 5HT can suppress phorbol ester-induced SERT phosphorylation and internalization, providing a mechanism to tune SERT capacity to the demands of 5HT release (34). Additionally, Jayanthi *et al.* (35) demonstrated a biphasic regulation of SERT by PKC in platelets, whereby initial SERT catalytic inactivation is followed by internalization correlated with distinct phosphorylation states. Recent reports also show that cell surface levels of SERT can be modified by protein kinase G (PKG) activation and p38 MAPK inactivation (36).

These initial studies suggest that the macromolecular organization of SERT protein complexes is differentially linked to specific SERT-associated membrane subdomains that in turn dictate SERT activity or mobility, and ultimately 5HT clearance capacity. We hypothesize that SERT inactivation and internalization is mediated by protein-protein associations that lead to active movement of the transporter through membrane skeleton/cytoskeleton domains. In the present study, using well established, differential extraction procedures (37–40), we analyze SERT distribution and localization in different cytoskeletal compartments upon exposure of platelets to 5HT, 5HT receptor agonists or phorbol esters. Most of the active plasma membrane SERT is associated with the membrane skeleton, whereas SERT appears to associate with the dense actin-cytoskeleton during inactivation and internalization. The translocation of SERT between these compartments is correlated with the interaction and translocation of the adaptor protein Hic-5. The interaction of Hic-5 with SERT can inactivate the transporter and facilitate SERT internalization through by promoting interactions with the actin cytoskeleton.

EXPERIMENTAL PROCEDURES

Preparation of Platelets—Outdated human platelet-rich plasma (PRP) was obtained from the American Red Cross. Studies with mouse platelets were performed in accordance with humane guidelines established by the Vanderbilt Institutional Animal Care and Use Committee (IACUC) under an approved protocol (M/04/376). Mouse platelets were collected in a tube containing acid-citrate-dextrose from the superior vena cava after sacrifice. Whole blood was centrifuged immediately at 190 × *g* for 15 min at room temperature to obtain platelet-rich plasma. The platelet-rich plasma was centrifuged at 2500 × *g* for 15 min at 22 °C, and the resulting platelet pellet was gently resuspended in phosphate-buffered saline (PBS) buffer, pH 7.4 and used immediately.

Immunocytochemistry and Confocal Microscopy—Glass coverslips were treated with collagen (100 μg/ml) for 4 h at 37 °C and washed three times with PBS. Human or mouse platelets were added at a 1×10^8 concentration and incubated at 37 °C for 15 min for adhesion. Platelets were then washed two times with PBS and fixed with 4% paraformaldehyde in PBS for 10 min at 4 °C, washed overnight with PBS and blocked with PBS solution containing 5% normal goat serum and 1% bovine serum albumin for 1 h at room temperature. Coverslips were then incubated overnight, at 4 °C with no. 48 affinity-purified rabbit anti-SERT antibody (30). The secondary anti-rabbit Alexa 680-conjugated antibody (Molecular Probes) was added after three washes with PBS and incubated for 1 h at room temperature. Three samples were used as negative controls to determine antibody specificity/background staining: SERT KO platelets, primary Ab alone and secondary Ab alone. The coverslips were then washed three times with PBS and mounted onto glass slides with aqua poly/mount (Polysciences, Inc., Warrington, PA). The samples were visualized using a laser scanning confocal microscope (Vanderbilt University Medical Center Cell Imaging Core Resource, LSM 510 META, Zeiss, Thornwood, NY).

Biotinylation of Platelets—Human or mouse platelets (1×10^9) were resuspended in room temperature assay buffer (150 mM NaCl, 2 mM $CaCl_2$, 10 mM triethanolamine, pH 7.8) containing 2.5 mg/ml sulfo-NHS-biotin (Pierce) and incubated for 40 min at 4 °C. The platelets were washed with ice-cold 50 mM Tris-HCl, pH 7.4 for 10 min at 4 °C and solubilized with radioimmune precipitation assay buffer (10 mM Tris, pH 7.4, 150 mM NaCl, 1 mM EDTA, 0.1% SDS, 1% Triton X-100, 1% sodium deoxycholate) containing protease and phosphatase inhibitors (1 μM pepstatin A, 250 μM phenylmethylsulfonyl fluoride, 1 μg/ml leupeptin, 1 μg/ml aprotinin, 10 mM sodium fluoride, 50 mM sodium pyrophosphate, and 1 μM okadaic acid). Surface-biotinylated proteins were isolated using streptavidin beads (Pierce). SERT levels from total extract, eluted fractions from streptavidin beads (surface-biotinylated fraction), and non-bound fractions (intracellular fractions) were analyzed by SDS-PAGE (10%), electroblotted to polyvinylidene difluoride membranes (Amersham Biosciences), and probed with SERT antibody (no. 48 rabbit affinity-purified antibody). Immunoreactive bands were detected by enhanced chemiluminescence (ECL; GE Healthcare Bio-Sciences Corp., Piscataway, NJ). Multiple film (CL-X Posure™, Pierce) exposures were obtained to ensure data capture in the linear range of film. Thereafter, the blots were stripped and probed with anti-actin monoclonal antibody (anti-β-actin, Sigma) and anti-Na^+/K^+-ATPase monoclonal antibody (Sigma) to validate surface biotinylation as well as equal protein loading and transfer. Band densities were quantified by integrating band density using computer-assisted densitometry (NIH Image 1.33u). Reported values represent absolute mean values ± S.E. (arbitrary units) of five or more independent experiments unless otherwise indicated.

Isolation and Analysis of Platelet Fractions—Platelet cytoskeletal fractions were isolated as previously described (18). Briefly, 10^8 platelets (human or mouse) were pelleted after pharmacological treatment by centrifugation at 5,000 × *g* for 2 min and lysed with 100 μl of 1% Triton X-100, 21 μM leupeptin, 2 mM phenylmethylsulfonyl fluoride, 20 μM pepstatin A, and 0.56 trypsin inhibitor unit/ml aprotinin in PBS, pH 7.4. Samples were resuspended and spun at 15,600 × *g* for 4 min at 4 °C in a bench top microcentrifuge for collection of cytoskeletal pellets (CS). The supernatants were transferred to a new tube and spun at 100,000 × *g* for 2 h (Beckmann M150 microultracentrifuge) for isolation of membrane skeleton (MS) pellets. The remaining supernatant was denominated TS (Triton-soluble) fraction. Each pellet was resuspended in 100 μl of RIPA buffer and either

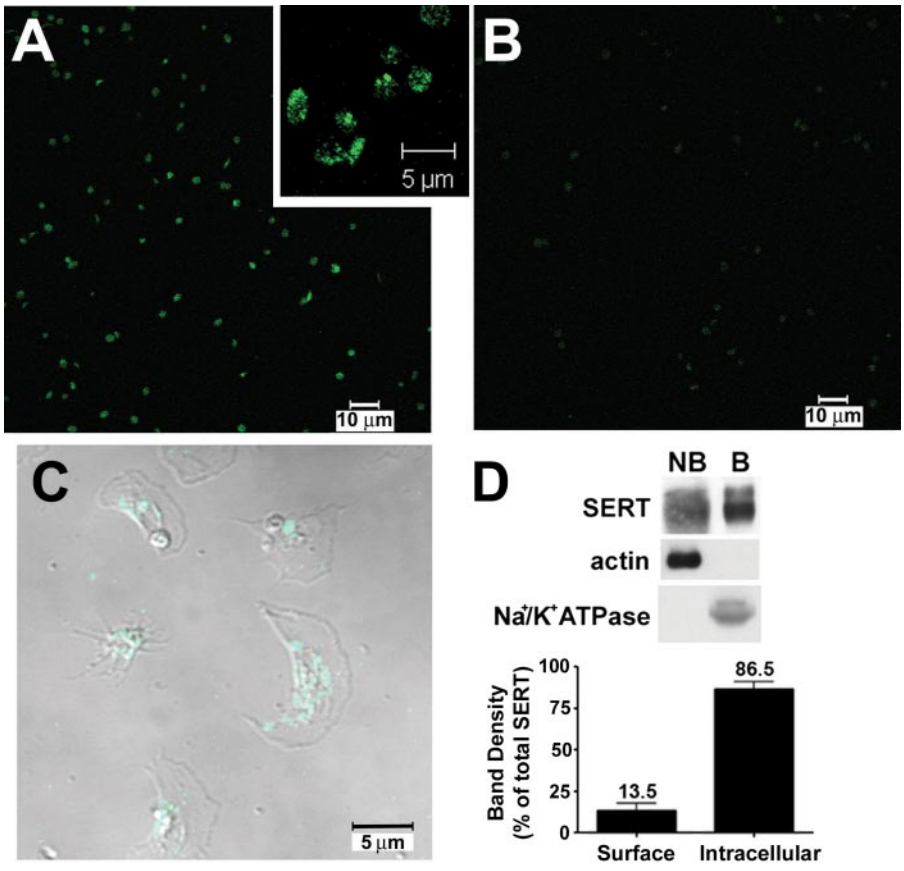

FIGURE 1. **Distribution of SERT in platelets.** *A–C*, immunocytochemistry and confocal microscopy of SERT in mouse and human platelets. SERT KO mouse platelets (*B*) show low background staining when compared with wild-type animals (*A*) under the same scanning conditions. *C*, human platelets show predominant intracellular SERT staining. *D*, SERT distribution as revealed by cell surface biotinylation. Mouse platelets were treated with sulfo-NHS-biotin as described under "Experimental Procedures." Purified proteins were probed with either anti-SERT polyclonal antibody (no. 48 serum) or anti-actin monoclonal antibody. *NB*, intracellular proteins (resistant to biotinylation) and *B*, surface (plasma membrane, or proteins that were biotinylated) proteins. Averaged data from eight independent experiments, normalized as percentage of total protein, are presented ± S.E. *NB* and *B* are statistically different ($p < 0.05$, Student's *t* test).

total content or equivalent protein amounts as described in the figure legends were subjected to 10% SDS-PAGE for Western blot analysis. Hic-5 and focal adhesion kinase (FAK) were detected on blots using monoclonal antibodies obtained from BD Transduction Laboratories (BD Biosciences, San Jose, CA) whereas anti-vinculin and anti-talin monoclonal antibodies were purchased from Sigma. Graphs that show arbitrary units were subsequently normalized to control values to assess percentage change over time/treatment (data cited under "Results"). For fractionation studies, each set of fractions (CS, MS, and TS) was analyzed independently as well as a fraction of total material in each sample where densities associated with CS+MS+TS = total protein. Statistical analyses were performed using GraphPad Prizm 4 software (GraphPad Software Inc.) using analysis of variance (ANOVA) or paired or unpaired Student's *t* tests as indicated under "Results."

Platelet Plasma Membrane Vesicle Preparation and 5HT Uptake—Resealed plasma membrane vesicles were isolated from human platelets according to Rudnick (41). Human platelet-rich plasma (25 ml) was treated with 10 μM 5HT or vehicle (PBS) for 30 min at 37 °C. Intact platelets were then collected by centrifugation at 10,000 × *g* for 10 min and lysed by washing three times with 10 mM Tris-HCl, 1 mM EDTA, 100 mM NaCl, pH 7.5, and loaded onto TENG buffer (80% (v/v) glycerol, 10 mM Tris, 1 mM EDTA, 100 mM NaCl pH 7.5). Platelet plasma membranes were purified by centrifugation at 15,600 × *g*, re-sealed in 1 ml of vesicle buffer (0.25 M sucrose, 10 mM Tris-HCl, 1 mM $MgSO_4$, and 1 mg of DNase) for 10 min at 37 °C and then purified by centrifugation at 17,000 × *g* for 2 h at 4 °C. The plasma membrane vesicles were resuspended in 0.25 M sucrose, 10 mM Tris-HCl, pH 7.5, at a concentration of 3–10 mg of membrane protein/ml, frozen in liquid nitrogen, and stored at −80 °C. Translation/transcription reactions containing either Hic-5 cDNA or control vector (see "Results") were added at this point and incubated with platelet membranes for 10 min at 37 °C during resealing of vesicles (TNT® quick-coupled transcription/translation systems, Promega, Madison, WI). The resealed vesicles were then frozen at −20 °C and purified the following day as mentioned above. Platelet plasma membrane vesicles (100 μg per tube) were resuspended in Krebs-Ringer's HEPES (KRH) buffer containing 130 mM NaCl, 1.3 mM KCl, 2.2 mM $CaCl_2$, 1.2 mM $MgSO_4$, 1.2 mM KH_2PO_4, 1.8 g/liter glucose, 10 mM HEPES, 100 μM pargyline, and 100 μM ascorbic acid. After 2 min of incubation with 50 nM [^{3}H]5HT (5-hydroxy[3H]tryptamine trifluoroacetate, 99.0Ci/mmol, Amersham Biosciences UK Limited, Buckinghamshire, UK), 5HT uptake was terminated by filtration through GF/B Whatman filters and washed three times with ice-cold KRH buffer. Filters were removed, immersed in scintillation fluid (Ecoscint™, National Diagnostics, Atlanta, GA) for ~8 h and quantitated by scintillation spectrometry. The counts obtained from the filtered samples were corrected for the nonspecific binding/uptake obtained by incubations with 1 μM paroxetine. Assay points were obtained in duplicate with cumulative uptake data arising from three or more independent experiments.

Immunoprecipitations—Immunoprecipitation and immunoblots were performed from detergent extracts of either human or mouse platelets, or mouse midbrain synaptosomes. Detergent extracts were prepared by washing 10^8 platelets with PBS and lysis by 1% Triton X-100 for 1 h at 4 °C. For SERT immunoprecipitations, 100 μg of protein extract was precleared with 5 μg of normal rabbit serum and 30 μl of 50% protein A-Sepharose bead slurry (Amersham Biosciences AB, Uppsla, Sweden) for 1 h at 4 °C. The precleared lysate was then incubated with either 1 μg of normal rabbit IgG or 1 μg of affinity-purified rabbit anti-SERT antibody

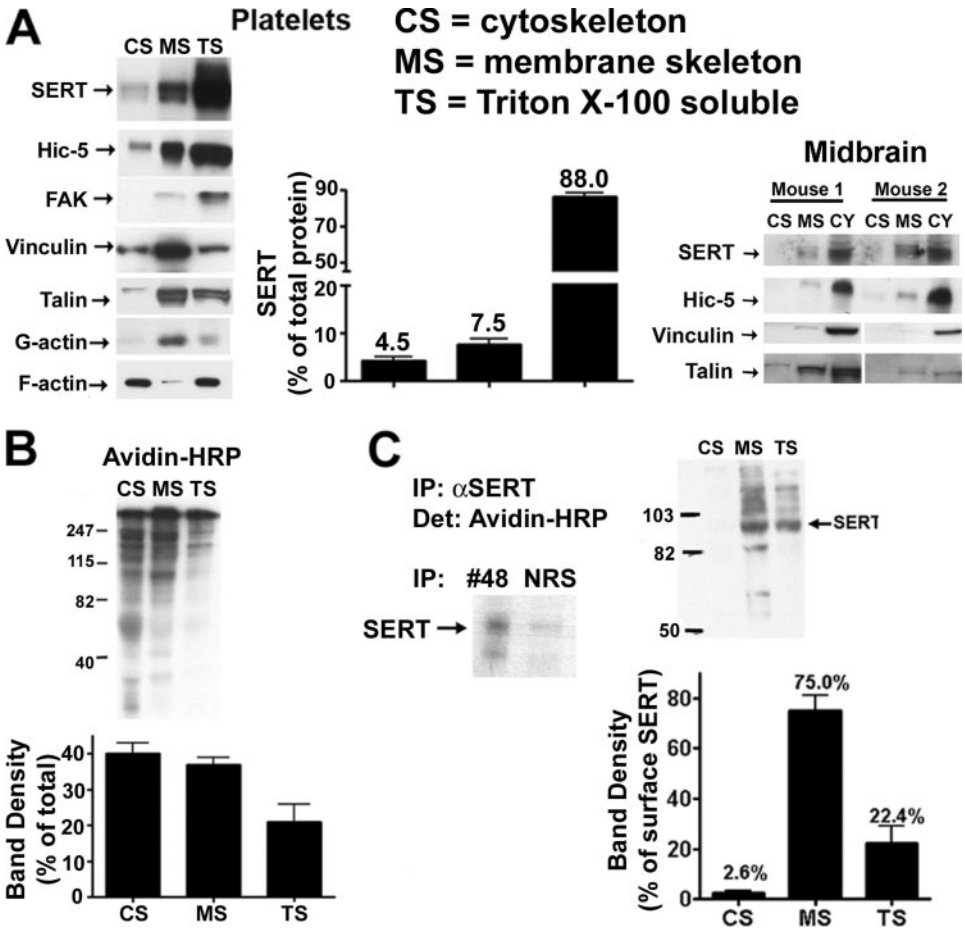

FIGURE 2. **Subcellular fractionation of platelets.** *A*, mouse platelet and midbrain cytoskeleton and membrane skeleton isolation. Mouse platelets were homogenized with PBS buffer containing 1% Triton X-100 and the CS, MS, and TS fractions were isolated as described under "Experimental Procedures." Equal volumes of each fraction were loaded and subjected to SDS-PAGE. Averaged data from eight independent experiments are presented ± S.E. *B*, distribution of plasma membrane proteins in the different platelet fractionations. Human platelets were biotinylated with sulfo-NHS-biotin and lysed with 1% Triton X-100, and CS and MS fractions were isolated. Equal volumes of each fraction were submitted to electrophoresis and plasma membrane proteins from each fraction were identified by blotting membranes with streptavidin-horseradish peroxidase (Amersham Biosciences). Data represent averaged densitometry from three independent experiments. *C*, distribution of the plasma membrane SERT between the different cytoskeletal compartments. Human platelets were biotinylated, and the CS and MS fractions were isolated. SERT was immunoprecipitated with no. 48 antibody, and plasma membrane SERT was identified as a 80-kDa streptavidin-horseradish peroxidase reactive band, absent from normal rabbit serum immunoprecipitates (see *inset*). Averaged data from three independent experiments are quantitated, revealing that the MS fraction contains most of the biotinylated SERT.

(purified from either no. 48 or no. 50 antisera, for details see Ref. 30) for 1 h at 4 °C followed by a 1-h incubation with 30 μl of a 50% protein A-Sepharose bead slurry at room temperature. Beads were then washed three times with PBS, and immunoprecipitated proteins were eluted in Laemmli buffer and analyzed by SDS-PAGE/Western blotting as described above.

RESULTS

Distribution of SERT in Platelets—An initial characterization of SERT membrane localization in platelets was assayed by immunocytochemistry (Fig. 1). We characterized SERT-specific staining in mouse platelets by using both wild-type (Fig. 1*A*) and SERT knock-out (Fig. 1*B*) mouse platelets and scanning with the same laser configuration for both samples. In wild-type samples, the majority of SERT immunoreactivity localizes to punctuate densities within intracellular compartments. We confirmed that most of the specific staining was also observed in intracellular compartments in human platelets, where almost no signal was detected at the plasma membrane (Fig. 1*C*). To define the relative abundance between surface and intracellular compartments we utilized cell surface biotinylation by incubating mouse platelets with cell-impermeable sulfo-NHS-biotin at 4 °C, followed by solubilization and collection of biotinylated platelet transporters on streptavidin beads (Fig. 1*D*). SERT immunoreactivity was evident in both plasma membrane (biotinylated, B) and intracellular (resistant to biotinylation or non-biotinylated, NB) fractions. Actin was restricted to the intracellular (NB) fractions, whereas the Na^+/K^+-ATPase was identified in the plasma membrane (B) fraction. Quantitative analyses demonstrates that the bulk of SERT protein is resistant to biotinylation (86.5 ± 4.5% intracellular, 13.5 ± 4.5% surface) indicative of substantial intracellular sequestration. Similar findings were obtained with human platelets (data not shown).

To better characterize SERT localization at both plasma membrane and intracellular compartments, we isolated MS and CS fractions by solubilization of mouse platelets. The procedure described under "Experimental Procedures" has been established to map protein translocation through skeletal compartments in human platelets following thrombin activation (39, 40, 42). The CS fraction isolated as a low speed (15,600 × *g*), Triton-X-100 insoluble fraction, is rich in filamentous actin and contains ~10% of total platelet proteins. The MS fraction requires high-speed (100,000 × *g*) centrifugation to pellet and is enriched for focal adhesion proteins such as vinculin and talin as well as other actin-binding proteins and also corresponds to ~10% of total proteins (18). The supernatant overlying the MS pellet that contains most platelet proteins (~80%) is denoted TS. We blotted the total content of these fractions and established that most of the SERT protein is present in the TS membranes (88.0 ± 1.7%) whereas only ~12% of total SERT protein resides in either the MS (7.6 ± 1.2%) or CS (4.4 ± 0.7%) membranes (Fig. 2*A*). Blotting for other marker proteins revealed the expected distributions for CS, MS, and TS fractions. For example, F-actin was localized to the CS fraction and depleted in the MS fraction, whereas the reverse is true for focal adhesion proteins (vinculin, talin). Focal adhesion kinase and Hic-5 predominated in the TS fraction, consistent with sizeable, soluble pools of these cytoplasmic proteins.

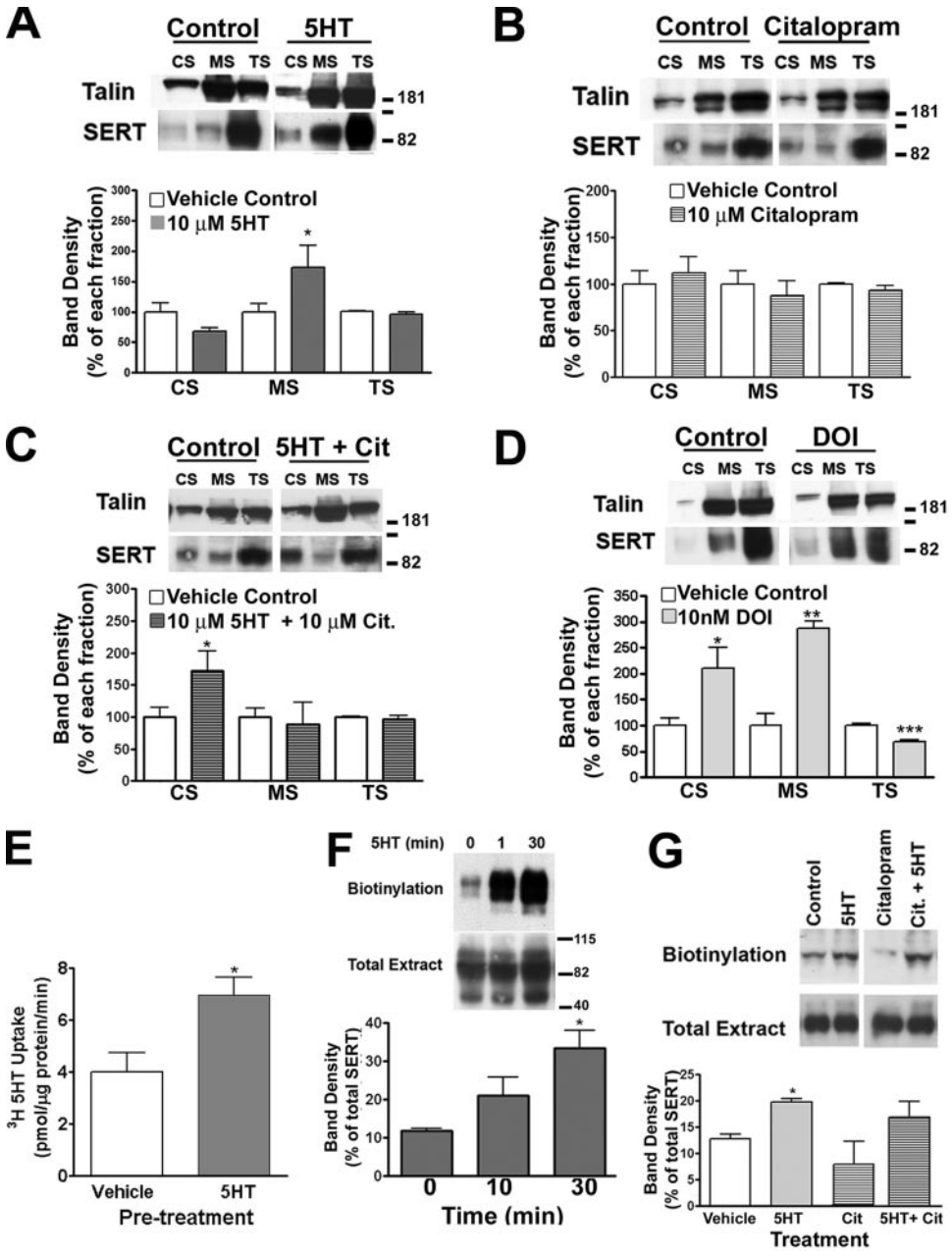

FIGURE 3. **5HT-induced redistribution of SERTs correlated with elevated 5HT uptake capacity.** *A–C*, SERT relocates to the MS fraction in the presence of 5HT. Mouse platelets were incubated for 30 min at 37 °C with either 10 μM 5HT (*A*) 1 μM citalopram (*B*), both (*C*), 10 nM DOI (*D*) or PBS (vehicle control), and CS and MS fractions were isolated. Data shown are representative of 3 (*A*), 4 (*B*), and 3 (*C* and *D*) independent experiments ± S.E. *E*, 5HT leads to an increase in the uptake activity of the SERT. Human platelets were incubated with 10 mM 5HT, and plasma membrane vesicles were prepared. Uptake was assessed by incubating 50 μg of vesicles with [3H]5HT as described under "Experimental Procedures." Averaged data from three independent experiments ± S.E. are presented. *, $p < 0.05$, unpaired Student's *t* test. *F*, time-course platelet biotinylation. Mouse platelets were incubated with 10 μM 5HT for increasing amounts of time at 37 °C followed by biotinylation at 4 °C. Plasma membrane transporters were identified by Western blot with the polyclonal anti-SERT antibody. Graph represents data average ± S.E. of four independent experiments (*, $p < 0.05$, paired Student's *t* test). *G*, human platelets were incubated with either 10 μM 5HT, 10 mM 5HT + 1 μM citalopram, 1 μM citalopram, or vehicle control at 37 °C followed by biotinylation at 4 °C. Membrane SERT was identified using affinity-purified no. 48 polyclonal antibody. Data presented show an average of three independent experiments (*, $p < 0,05$, paired Student's *t* test).

To determine how TS, MS, and CS fractions relate to SERT distribution defined by biotinylation, we biotinylated platelets prior to cell fractionation, and then examined fractions for evidence of biotinylation using avidin-HRP In Fig. 2*B* we show that the bulk of plasma membrane proteins are localized to either the CS or the MS fractions (77 ± 7.1% for MS+CS) indicating that the bulk of the TS fraction derives from intracellular proteins and membrane compartments. Interestingly, although CS and MS fractions exhibit an equivalent level of total biotinylated proteins, SERT was not evenly distributed between CS and MS fractions (Fig. 2*C*). When the biotinylated CS and MS fractions were immunoprecipitated with SERT antibodies, significantly more biotinylated material was recovered from the MS fraction, suggesting that most of the SERT in the CS fraction is internalized or otherwise inaccessible to biotinylation. Looking at the relative distribution across biotinylated fractions, SERT in the MS fraction constituted 81.7 ± 10.2% of total surface SERT protein. This distribution is unlikely to be caused by a problem with antibody access to CS or MS fractions by SERT antibodies used for immunoprecipitation as we recovered SERT equivalently when CS and MS sample input was balanced for SERT abundance (data not shown). These findings indicate that under basal conditions, the bulk of platelet SERT resides in intracellular, TS membranes, whereas the fraction of SERT that is resident at the plasma membrane is enriched in the MS fraction.

5HT-induced Redistribution of SERT—The ability of substrates and antagonists to regulate endogenous SERT surface expression has been demonstrated via biotinylation experiments on transporter-transfected cells and cultured neurons (34). To initiate an analysis of how the cytoskeleton might participate in these effects, we sought to determine whether exposure of platelets to exogenous 5HT changes the differential distribution of SERT that we have established through extraction/sedimentation. We performed differential extractions on mouse platelets preincubated (30 min) with 10 μM 5HT at 37 °C. Although the overall distribution of talin remained the same under these conditions, we observed a significant increase in SERT in the MS fraction (Fig. 3*A*, 1.72 ± 0.36-fold; $p < 0.05$, unpaired Student's *t* test). With this treatment, we also consistently observed a small reduction of SERT in the CS fraction although this change did not reach statis-

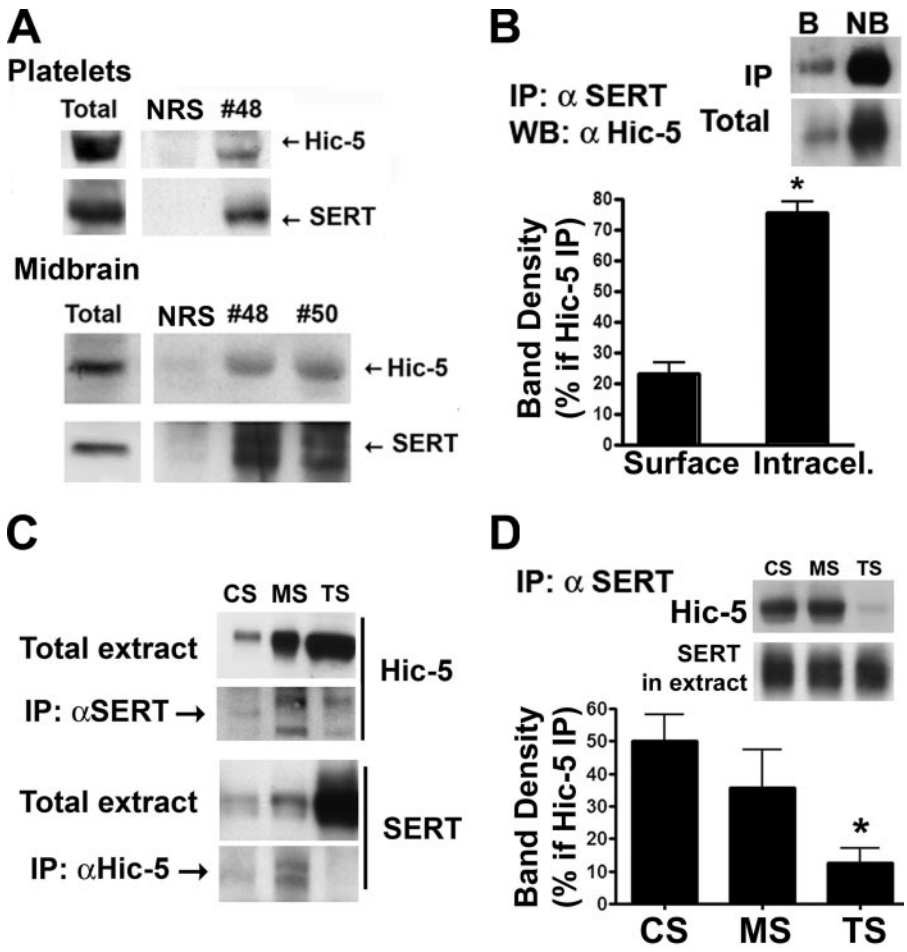

FIGURE 4. **Hic-5 interacts with SERT in platelets.** *A*, immunoprecipitation of SERT and identification of Hic-5 as a SERT-interacting protein in human platelets and mouse midbrain synaptosomes. 100 μg of tissue was incubated with either rabbit serum (*NRS*) or SERT-specific rabbit serum (no. 48 and no. 50) and purified by the addition of protein A-Sepharose. Immunoblots were probed with either the monoclonal Hic-5 antibody or monoclonal anti-SERT antibody. *B*, Hic-5 largely interacts with intracellular pools of SERT. Human platelets were biotinylated, and the plasma membrane proteins purified. SERT was immunoprecipitated from both biotinylated and non-biotinylated samples, and Hic-5 was identified by Western blot. Data represent the average ± S.E. of 8 experiments (*, $p < 0.0001$, paired Student's *t* test). *C*, Hic-5/SERT interaction occurs mostly in association with the membrane skeleton. Hic-5 or SERT immunocomplexes were isolated from equal volumes of CS, MS, and TS fractions previously isolated. Immunocomplexes isolated with the anti-Hic-5 antibody were submitted to SDS-PAGE, and membranes were blotted with anti-SERT antibody (no. 48). SERT immunocomplexes were also submitted to SDS-PAGE, and Hic-5 was identified. Western blots show a representative experiment of five independent experiments. *D*, TS SERT is not associated with Hic-5. Mouse platelets were fractionated, and volumes were normalized for equal amounts of SERT (see SERT in extract). SERT-associated immunocomplexes were purified and Hic-5 identified by Western blot. Averaged data from three independent experiments are presented as percentages of total Hic-5 associated with SERT.

tical significance. No apparent change was evident in the TS fraction. Although these data suggest a movement of CS SERT protein to the MS fraction, other interpretations are possible because these are steady-state measurements and the TS fraction is significantly more populated, diminishing sensitivity to detect small changes in this pool. To test whether the changes observed are caused by 5HT interacting with SERT or to platelet 5HT2A receptors, we repeated our 5HT fractionation studies in the presence of 1 μM citalopram, a high-affinity SSRI (Fig. 3, *B* and *C*). Citalopram alone induced no significant changes in SERT distribution, although we noticed a trend toward a decrease in MS and increase in CS levels (Fig. 3*B*). Importantly, the SSRI totally antagonized the increase in MS SERT triggered by 5HT (Fig. 3*C*). With the combination of 5HT and SSRI, we also observed a significant increase of SERT in the CS fraction (1.72 ± 0.31-fold; $p < 0.05$, unpaired Student's *t* test). This increase is probably because of 5HT2A receptor activation by 5HT, supported by experiments using 10 nM of the 5HT2A receptor agonist DOI (Fig. 3*D*). This concentration was able to trigger SERT translocation from TS fractions to both MS and CS fractions (CS, 2.09 ± 41.51-fold, $p < 0.05$; MS, 2.87 ± 14.22-fold, $p < 0.005$; TS, 32.40 ± 5.158% reduction, $p < 0.001$). To explore whether the 5HT-induced increase of SERT protein in the MS fraction is paralleled by changes in SERT uptake capacity, we preincubated human platelets with 10 μM 5HT for 30 min at 37 °C and then prepared platelet membrane vesicles to assess SERT activity (41). In these studies (Fig. 3*E*), we observed an ~70% increase in SERT uptake in platelets pre-incubated with 5HT as compared with vehicle (173.8 ± 17.6% of vehicle, $p < 0.05$, unpaired Student's *t* test). Because these changes could also be associated with a 5HT-induced redistribution of SERT to the plasma membrane, we assessed the impact of 5HT on platelet SERT surface density via biotinylation we obtained evidence of a time-dependent elevation in surface SERT (Fig. 3*F*). However, unlike changes in SERT membrane fractionation, the effect of 5HT on surface trafficking was not reversed by co application of 1 μM citalopram (Fig. 3*G*). Taken together, these data suggest that 5HT is able to trigger SERT translocation to the plasma membrane expression and MS translocation. This translocation seems to be triggered by 5HT2A receptor activation and is dependent on SERT activity.

Association of SERT with the Membrane Skeleton Adaptor Protein Hic-5—The MS fraction contains multiple actin-binding and signaling proteins that could interact with SERT and regulate its function and localization. Hic-5 is a multiple LIM-domain protein previously identified as a DAT-interacting protein via yeast 2-hybrid studies, interactions validated in heterologous systems as well as in striatal synaptosomes. The SERT C terminus was previously shown to interact directly with Hic-5 via yeast two-hybrid experiments (32), although to date no validation of this interaction has been established with native preparations. Importantly, Hic-5 is expressed in platelets (43, 44). Immunoprecipitations of total platelet extracts with SERT antisera (no. 48) but not normal rabbit serum, lead to Hic-5 co-immunoprecipitation (Fig. 4*A*). We also

found evidence of a SERT·Hic-5 complex with detergent extracts of mouse midbrain synaptosomes using two different SERT antisera (no. 48 and no. 50) (Fig. 4*A*). Next we asked whether Hic-5 was associated with surface or intracellular SERT (Fig. 4*B*). Although we recovered most Hic-5 from intracellular (NB) SERT samples, detectible quantities of Hic-5 were identified in plasma membrane (B) extracts (23.4 ± 3.3% of total recovered). Consistent with these findings, we found Hic-5 predominantly associated with TS fractions (84.9 ± 3.3%) with a smaller, but readily detectable quantity in MS fractions (13.9 ± 3.1%). We then investigated the possibility of a link between SERT·Hic-5 complex interactions and specific fractions. Whether using total material recovered from each fraction (Fig. 4*C*) as input for co-immunoprecipitation or using as input samples balanced for SERT abundance (Fig. 4*D*), we observed a significant deficit in SERT/Hic-5 interactions in the TS fraction. As we can readily recover SERT from all three fractions (data not shown), these findings indicate highly preferential interactions of Hic-5 with MS- and CS-associated SERT.

Regulation of SERT/Hic-5 Interaction by 5HT—Our evidence of a selective association of SERT with Hic-5 in the CS and MS fractions as opposed to the largely cytoplasmic TS fraction suggested to us that Hic-5 might play an important role in activity-dependent changes in SERT membrane redistribution/catalytic activity. We asked whether 5HT treatment of platelets (10 μM 5HT, 30 min) alters recovery of SERT·Hic-5 complexes through co-immunoprecipitation assays. Whereas 5HT did not alter total Hic-5 levels, we observed a significant decrease in SERT/Hic-5 associations relative to vehicle treatments (Fig. 5*A*). Citalopram alone yielded a significant increase in SERT/Hic-5 associations, which remained similarly elevated when citalopram and 5HT were co applied. Importantly, 5HT lost the ability to trigger a SERT/Hic-5 dissociation in the presence of the SSRI, indicating that SERT activity and/or ligand binding influence the interactions of these two proteins. We then asked whether 5HT alters Hic-5 distribution between membrane subfractions. Platelets were treated with vehicle or 5HT (10 μM, 30 min), TS, CS, and MS fractions generated and blotted in parallel for SERT and Hic-5 (Fig. 5*B*). We observed an enrichment of Hic-5 in MS fractions concomitant with a decrease in the TS fraction ($p < 0.01$ for MS and TS; unpaired Student's *t* test). These findings establish three actions of 5HT: 1) to translocate SERT to the plasma membrane, 2) to alter the subcellular distribution of SERT and Hic-5, elevating both in the MS fraction, and 3) to diminish SERT/Hic-5 associations.

Regulation of SERT/Hic-5 Interaction by PKC Activation—The data acquired in 5HT studies are consistent with SERT capacity increasing in parallel with a loss of SERT·Hic-5 complexes. Do SERT/Hic-5 associations increase in parallel with stimuli triggering SERT down-regulation? The best characterized stimuli for rapid SERT down-regulation are phorbol esters that activate PKC (34, 45). Consistent with prior studies, incubation of mouse platelets with β-PMA (1 μM, 37 °C) led to a time-dependent decrease in the abundance of SERT proteins at the cell surface as assessed by biotinylation ($p < 0.05$, paired Student's *t* test, Fig. 6*A*). To test whether the interaction between SERT and Hic-5 is modulated by PKC, we co-immunoprecipitated SERT following treatment of mouse platelets

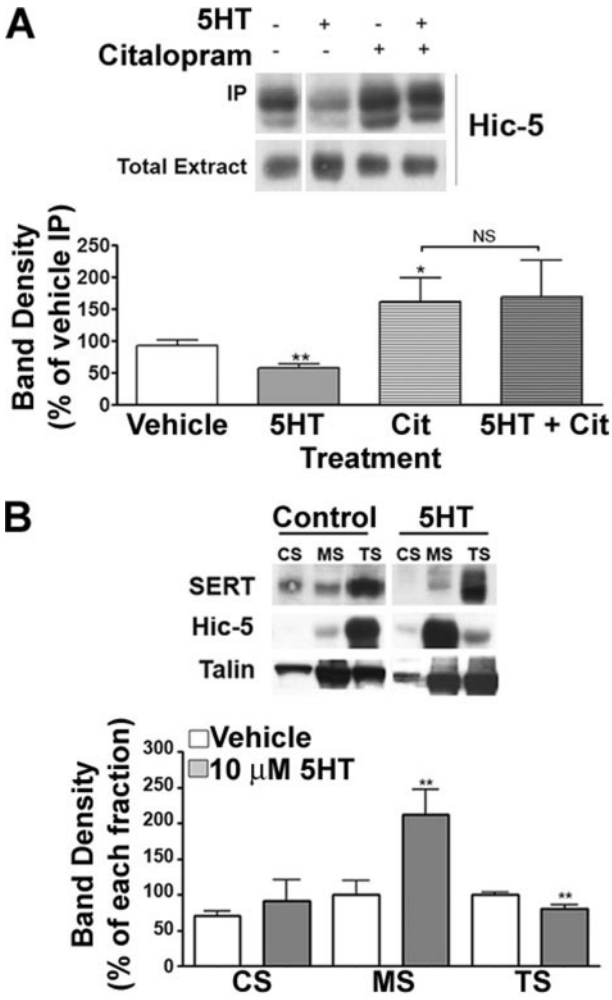

FIGURE 5. **Hic-5/SERT interactions are regulated by 5HT.** *A*, immunoprecipitation of SERT from mouse platelets. Mouse platelets were incubated with either 10 mM 5HT, 1 μM citalopram, 1 μM citalopram + 10 μM 5HT, or PBS (vehicle control) for 30 min at 37 °C, and SERT was immunoprecipitated as described under "Experimental Procedures." Averaged data from four independent experiments are presented ± S.E. (*, $p < 0.05$ and **, $p < 0.01$, paired Student's *t* test). *B*, translocation of Hic-5 between the different cytoskeletal compartments in the presence of 5HT. Mouse platelets were incubated with 10 μM 5HT, lysed with 1% Triton X-100, and the CS and MS pools were purified by differential fractionation. Averaged data of three independent experiments are presented.

with 1 μM PMA for 30 min at 37 °C. As shown in Fig. 6*B*, β-PMA triggered a significant, ~50% increase in the abundance of SERT·Hic-5 complexes ($p < 0.05$, paired Student's *t* test). We did not observe any changes in Hic-5 total levels in the presence of β-PMA. The effect of β-PMA was completely antagonized by the specific PKC antagonist bisindolylmaleimide (BIM; 1 μM). Further analyses of the impact of β-PMA revealed that SERT·Hic-5 complexes form in a delayed manner, with significant elevations requiring 10–30 min of stimulation (Fig. 6*C*) and were most evident in dose response studies at higher concentrations of β-PMA (Fig. 6*D*).

Osada *et al.* (46) have demonstrated that Hic-5 translocates from MS fractions to CS compartments upon platelet activation with thrombin. Because PKC is one of the protein kinases activated after thrombin stimulation, we sought to establish whether Hic-5 also translocates under conditions of β-PMA treatment that leads to enhanced SERT·Hic-5

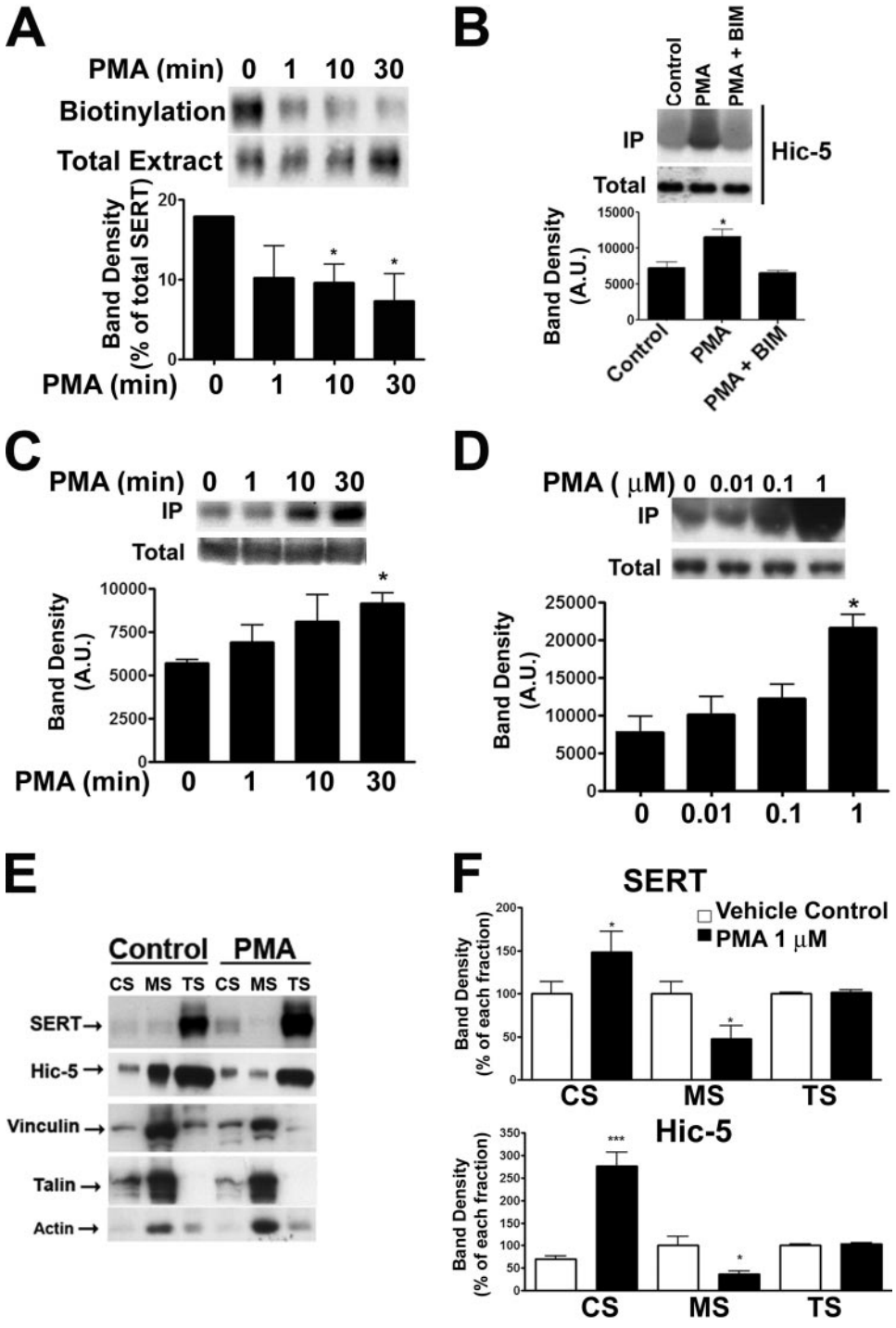

FIGURE 6. **SERT surface density and Hic-5/SERT interactions are regulated by PKC activation.** *A*, time course platelet surface biotinylation. Mouse platelets were incubated at 37 °C with 1 μM β-PMA for increasing times and surface proteins were biotinylated at 4 °C and isolated. Plasma membrane transporters were identified by Western blot with the polyclonal anti-SERT antibody. Graph represents data average ± S.E. of four independent experiments (*, $p < 0.05$, paired Student's *t* test). *B*, immunoprecipitation of SERT from mouse platelets. Mouse platelets were incubated with either 1 μM β-PMA, 1 μM β-PMA + 1 μM BIM or PBS (vehicle control) for 30 min at 37 °C, and SERT was immunoprecipitated as described under "Experimental Procedures." Averaged data from three independent experiments are presented ± S.E. (*, $p < 0.05$, paired Student's *t* test). Shown are time course (*C*) and concentration curve (*D*) of β-PMA effect onto the SERT/Hic-5 association. Mouse platelets were incubated for increasing times (*C*) and increasing concentrations (*D*) of β-PMA, and SERT was immunoprecipitated. Averaged data of 4 (*C*) and 3 (*D*) experiments are presented. *E* and *F*, translocation of SERT and Hic-5 between the different cytoskeletal compartments in the presence of β-PMA. Mouse platelets were incubated with 1 μM β-PMA, lysed with 1% Triton X-100, and the CS and MS pools were purified by differential centrifugation. *E*, averaged data of three independent experiments are presented ± S.E. (unpaired Student's *t* test: *, $p < 0.05$; ***, $p < 0.001$).

complexes. After incubation with 1 μM PMA for 30 min we observed a dramatic change in Hic-5 distribution with a nearly 3-fold increase in Hic-5 associated with the CS fraction and a concomitant decrease in the percentage of total Hic-5 present in the MS fraction (Fig. 6, *E* and *F*). An analysis of SERT surface expression and SERT/Hic-5 interaction revealed that increasing Hic-5 associations correlate inversely with surface levels of SERT (Pearson $r_s = -0.92$, $r^2 = 0.85$). We therefore asked whether β-PMA also triggers a parallel redistribution of SERT between CS and MS fractions. Indeed, blotting fractions derived from β-PMA treated platelets revealed a 1.5-fold elevation of SERT in the CS fraction and a 2-fold decrease in the MS fraction (Fig. 6, *E* and *F*). This redistribution could also be observed using surface fractions derived from biotinylation prior to fractionation (data not shown).

5HT, acting through SERT, has been shown to inhibit SERT phosphorylation and endocytosis triggered by PKC (47). We thus asked whether 5HT would attenuate the β-PMA-induced changes in SERT and Hic-5 subcellular distributions as well as the phorbol ester triggered elevation in Hic-5·SERT complexes. We incubated mouse platelets with 1 μM β-PMA and 10 μM 5HT or vehicle for 30 min. at 37 °C and fractionated platelets as described above. We found that coincubation of β-PMA with 5HT blocked the changes in SERT subcellular distribution induced by phorbol ester (Fig. 7, *A* and *B*). In contrast, 5HT exerted no effects on Hic-5 protein distribution between CS, MS, and TS compartments. 5HT treatments also abolished the phorbol ester-mediated increase in SERT·Hic-5 complexes as revealed by co-immunoprecipitation experiments (Fig. 7*C*).

β-PMA treatments have been found to trigger both an inactivation and endocytosis of SERT proteins (48). Although SERT/Hic-5

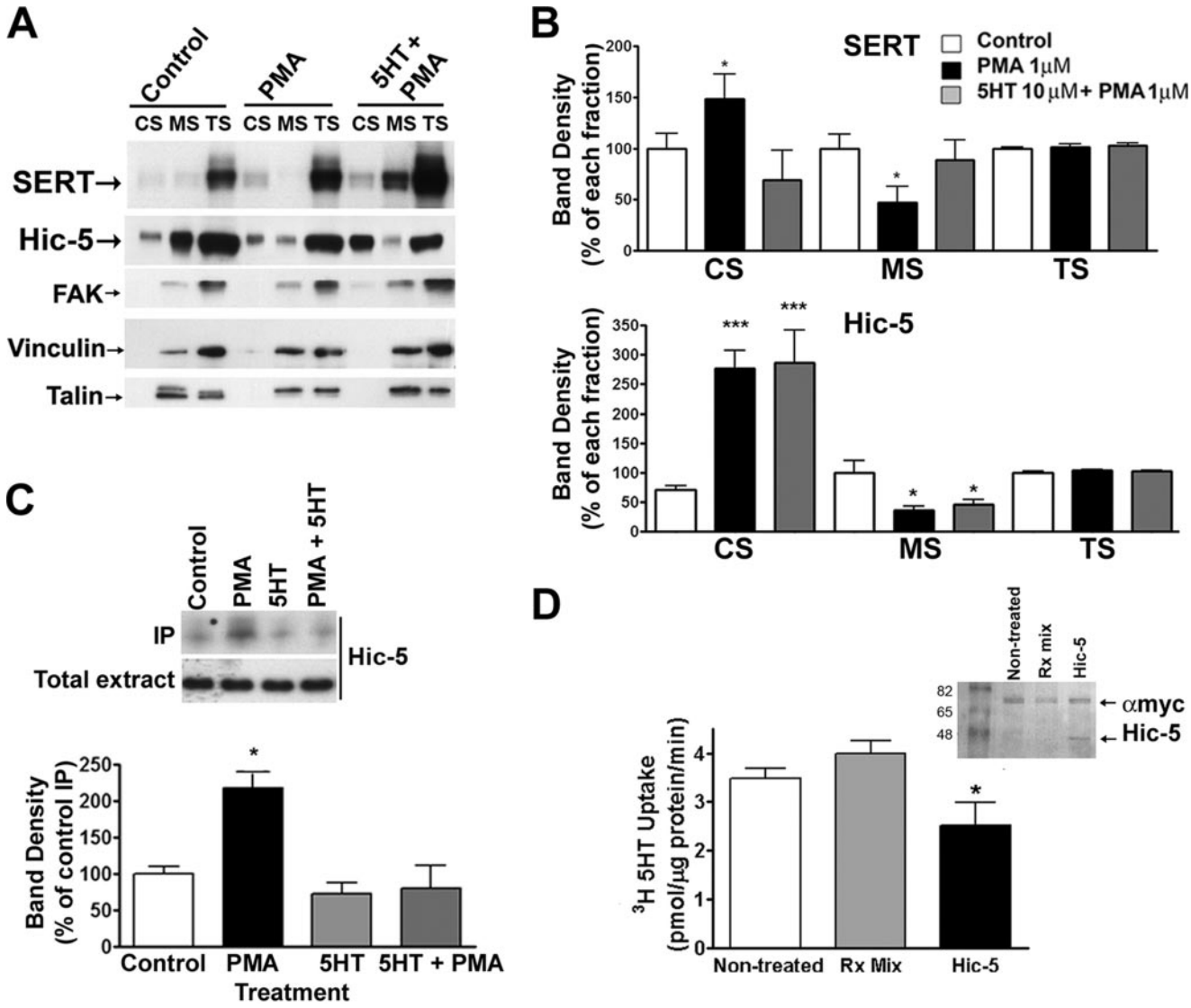

FIGURE 7. **5HT attenuates the β-PMA-induced changes in SERT and Hic-5 subcellular distribution and Hic-5·SERT complexes.** *A* and *B*, platelet fractionation. Mouse platelets were incubated with either 1 μM PMA, 1 μM PMA + 10 μM 5HT, or vehicle control for 30 min at 37 °C and cytoskeletal fractions (CS and MS) isolated. Data in *B* show an average of four independent experiments ± S.E. *C*, immunoprecipitation of SERT. Mouse platelets were treated as described in *A* and SERT was immunprecipitated. Hic-5 was identified using the monoclonal anti-Hic-5 antibody. Data presented are an average of four independent experiments ± S.E. *D*, uptake in platelet plasma membrane vesicles containing Hic-5. Human platelets plasma membranes were prepared and re-sealed in the presence of *in vitro* transcribed-Hic-5 (*Hic-5*), the transcription reaction mix alone (*Rx mix*) or in the presence of vesicle buffer alone (non-treated), incubated for 10 min at 37 °C and then frozen at −20 °C for 16–18 h. Approximately 25 μg of resealed plasma membrane vesicles were used for [^{3}H]5HT uptake experiments. Graph represents averaged data of four independent experiments, conducted in triplicates (* = $p < 0.05$, Student's *t* test). *Inset*, colloidal *blue staining* of the translation product from the *in vitro* translation reaction. Each reaction was incubated with anti-Myc monoclonal antibody, and immunoprecipitates were submitted to 12% SDS-PAGE. Colloidal blue staining reveals a ~48-kDa band, corresponding to the translation product (Hic-5).

associations occur at a dose/time most related to changes in SERT surface distribution, elevated Hic-5/SERT interactions might also stabilize a less active state of SERT triggered by phorbol ester. To eliminate concerns for effects of Hic-5 on trafficking *per se*, we transcribed and translated Hic-5 *in vitro* and incubated product with purified human platelet membranes prior to resealing them for transport studies. As a control, we used vesicles sealed in the presence of the control transcription/translation reaction mix, (which contains the RNA polymerase complex, reticulocyte lysates and luciferin). In comparison to vehicle or non-treated controls, we observed a 30% decrease in SERT activity with Hic-5 translation product (Fig. 7*D*; 63.1 ± 11.7%, $p < 0.05$, paired Student's *t* test). These findings suggest that association of SERT with Hic-5 may also participate in catalytic activity modulation of SERT function.

DISCUSSION

Plasma membranes in eukaryotic cells are organized into domains of specialized functions. Many of these domains are relatively stable at the cell surface and involve a series of linkages between cytoplasmic cytoskeletal proteins, integral membrane proteins and extracellular attachments to the substrate or to other cells (15). The platelet membrane skeleton is a lattice-like structure that coats the plasma membrane, composed of short actin filaments, spectrin, vinculin, and other focal adhesion proteins (13). The platelet cytoskeleton is composed of filamentous actin

(F-actin) as well as microtubules that coil around the cell periphery immediately beneath and parallel to the plasma membrane (49). Hartwig and DeSisto (50) demonstrated that the long actin fibers make connections with the membrane lamina through the intermediary of actin-binding protein, and at one end, with the surface and margins of the membrane skeleton. Even though the membrane skeleton is anchored to the F-actin fibers in the intact platelet, it is possible to mechanically separate those two components of the cell. Because SERT is under regulation by multiple signaling pathways that positively and negatively regulate surface expression and intrinsic activity, we capitalized on differential extraction techniques to monitor protein associations with SERT and its own movements in and out of these fractions.

In our study, we provide evidence that SERT is a membrane skeleton-associated protein that, upon inactivation, associates with the cytoskeleton followed by internalization. As a membrane skeleton member, the adaptor protein Hic-5 is also a SERT-interacting protein. This interaction occurs in low but detectable levels in resting platelets, and the SERT·Hic-5 complex was localized to intracellular compartments, although a small population of plasma membrane SERT is associated with Hic-5. Surprisingly, most of the SERT·Hic-5 complex is not present in the Triton X-100 fraction, which contains most of the SERT and Hic-5 (>80% of total proteins), but rather exists in association with both cytoskeleton and membrane skeleton. These data are consistent with the role of Hic-5 as an adaptor protein that translocates from focal adhesions to actin-cytoskeleton components upon mechanical stretching in fibroblasts (51).

We propose that Hic-5 associates with SERT only as the transporter transits to the cytoskeleton, where it may eventually endocytose (Fig. 8). Once SERT containing vesicles have budded from the plasma membrane, Hic-5 may dissociate, leading to the large pool of intracellular SERT present in the TS fraction but devoid of Hic-5 interactions. Our conclusions are tempered by the fact that the methods we have employed do not permit direct monitoring of SERT (or Hic-5) as it moves between compartments. Possibly, a large and relatively immobile TS pool of SERT containing vesicles could be devoid of Hic-5 whereas a small recycling pool of SERT vesicles could retain Hic-5 associations, accounting for a small amount of recovery of SERT·Hic-5 complexes from TS fractions. Further studies that incorporate dynamic monitors of trafficking and protein associations should aid in this analysis.

Regardless of the limitations noted above, our studies denote a dynamic profile of SERT/Hic-5 associations in platelets that likely has important consequences for transporter trafficking and the macromolecular organization of additional SERT regulatory proteins. Hic-5 is known to participate in regulated pathways linked to platelet activation. Osada *et al.* (46) have described Hic-5 tyrosine phosphorylation and translocation during platelet activation induced by thrombin stimulation, suggesting that PKC regulates Hic-5 phosphorylation in an indirect manner. Our observation that Hic-5 translocates to cytoskeletal structures upon PKC activation is consistent with the idea that PKC changes Hic-5 localization and, reasonably, such effects appear to be SERT-independent. Nonetheless, we have observed a time and concentration-dependent increase in

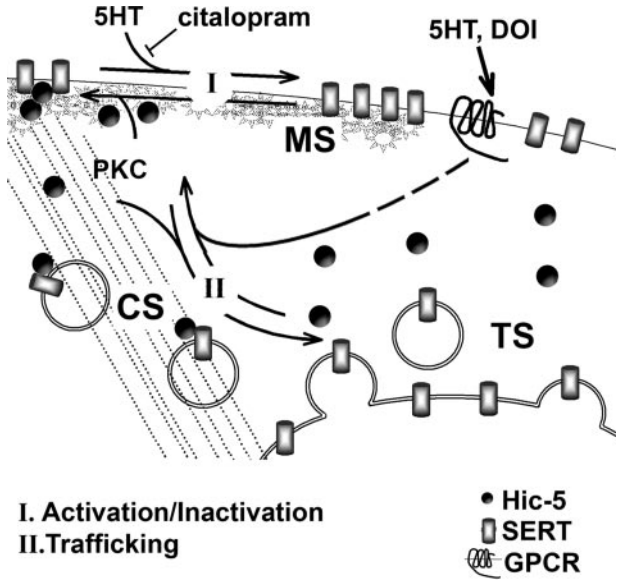

FIGURE 8. **A model for the regulated translocation of SERT.** The bulk of the platelet SERTs are localized in intracellular, Triton X-100 soluble fractions. 5HT mediates the translocation of intracellular SERTs to the plasma membrane associated with the membrane skeleton. The activation and MS localization of SERT are inhibited by citalopram, leading to an accumulation of SERTs in the cytoskeletal-associated fractions and concomitant increase in associations with Hic-5 (CS). The activation of PKC by PMA induces SERT/Hic-5 associations leading to inactivation and translocation to the CS followed by internalization. Both of these processes are inhibited by 5HT.

the SERT/Hic-5 association after PKC activation that correlates with transporter internalization. We propose that SERT internalization is initiated through, in part, its association with Hic-5 and translocation to the cytoskeleton while still at plasma membrane, followed by internalization. Activation of PKC in platelets produces a biphasic regulation of the transporter, involving a rapid (1 min) loss of transport activity followed by a more delayed (10–30 min) loss of surface SERT, correlated respectively with phosphorylation of serine and threonine residues (35). Our time course and dose response studies are more indicative of Hic-5 participating in later stages of SERT regulation, though possibly Hic-5 may trap transporters shifted to a less active state.

The increase of SERT in the cytoskeletal fraction during PKC activation might reflect the association of SERT-containing vesicles with the actin microfilaments during endocytosis. This association does not seem to be permanent, as indicated by the high levels of intracellular SERT present in the TS fraction, though the mobility of the latter fraction has not been studied explicitly. Regardless, our data indicate that intracellular SERT-containing vesicles are predominantly cytoskeleton-free. Whether the transport of SERT to the plasma membrane involves an association with microfilaments is still unknown, although this type of association has already been described for the glutamate transporter, where the disassembly of actin filaments by cytochalasin D blocked the expected increase of transporters at the cell surface induced by insulin (42, 52). Because SERT·Hic-5 complexes do not accumulate in intracellular TS membranes, we suggest that Hic-5 is not responsible for "trapping" SERT inside the cell, but rather for either accelerating endocytosis or possibly reducing recycling rates. Fur-

ther studies using peptide inhibitors of Hic-5/SERT interactions or genetic manipulations to interfere with Hic-5 associations should be helpful in this regard.

Two basic mechanisms are evident for how interactions with the actin cytoskeleton may regulate SERT function. First, association with the cytoskeleton may change transporter intrinsic transport rates and second, these associations may allow for a precise localization and clustering of the transporter in specific membrane subdomains. Studies in SERT-expressing COS-7 cells that were exposed to cytochalasin D reported a decrease in SERT uptake activity, indicating that the integrity of the actin cytoskeleton is necessary for supporting SERT function (53). Our data support the notion that both active and inactive plasma membrane transporters are associated with the membrane skeleton, where Hic-5 might connect SERT with actin fibers. We suggest that SERT associations with these elements may change in an activity-dependent manner as evidenced by the ability of 5HT to alter SERT subcellular distribution in an antidepressant-sensitive manner. Recent findings show that the SERT carboxyl terminus can attenuate transporter activity by functioning as a molecular decoy that disrupts the interaction of SERT with components of the actin cytoskeleton (54). The authors speculate that excess C termini would disturb the proper SERT anchoring to actin cytoskeleton via SERT accessory proteins such as MacMARCKS. The interaction of SERT with Hic-5 we have described, on the other hand, seems to diminish SERT intrinsic uptake activity (Fig. 7*D*), and this interaction appears to be negatively influenced by SERT activity and positively by PKC activation. Hic-5 may compete with other proteins like MacMARKS that stabilize SERT localization to the MS leading to SERT inactivation and eventually transporter endocytosis.

Finally, we wish to note the possibility that SSRIs may alter several facets of SERT regulation. We established that 5HT induces a relocation of SERT to the MS in a citalopram-sensitive manner and that 5HT-induced reductions in SERT·Hic-5 complexes were also blocked by the antidepressant. In contrast, the ability of 5HT to trigger elevated surface expression appears to be related to other actions of the amine, such as 5HT2A receptor stimulation. In fact, the 5HT2A agonist DOI induces an increase of SERT in both cytoskeleton and membrane skeleton fractions, suggesting a regulated exocytosis mechanism. Regardless, either directly or indirectly, several facets of SERTs regulation appear to be influenced by transport activity, including SERT associations with regulatory proteins. Previously, we documented that 5HT could attenuate phorbol ester induced changes in SERT phosphorylation (47) as well as PP2A associations (30). Here we add associations with Hic-5 to this growing list. We do not know the primary mechanism by which 5HT translocation influences associations and redistribution. Multiple mechanisms appear tenable. For example, transporter conformations associated with 5HT uptake may facilitate movements between cytoskeleton and membrane skeleton compartments. Alternatively, 5HT-gated currents (28) or intracellular 5HT accumulation may indirectly influence these phenomena. Finally, transport-related conformations may impact access of transporters by phosphatases and kinases whose activities may alter SERT phosphorylation status, driving these phenomena. We also observed some intrinsic activity of citalopram, generally yielding effects opposite those of 5HT. This may reflect stabilization of transport-incompetent conformations of the protein or limit indirect effects of 5HT on host cells. Examination of the properties of different classes of antidepressants to influence subcellular localization and SERT heteromeric assemblies may offer additional insights into the distinct therapeutic profiles of SSRIs.

Acknowledgments—We thank Tammy Jessen and Angela Steele for the expert support in general laboratory maintenance, Qiao Han for antibody development, and Jane Wright in animal husbandry. We gratefully acknowledge the use of the Vanderbilt University Medical Center Cell Imaging Core Resource (supported by National Institutes of Health Grants CA68485 and DK20593). We thank Alicia Ruggiero for critical review of the manuscript.

REFERENCES

1. Torres, G. E., Gainetdinov, R. R., and Caron, M. G. (2003) *Nat. Rev. Neurosci.* **4,** 13–25
2. Pollock, B. G. (2001) *Expert Opin. Pharmacother* **2,** 681–698
3. Murphy, D. L., Lerner, A., Rudnick, G., and Lesch, K. P. (2004) *Mol. Interv.* **4,** 109–123
4. Murphy, D. L., Uhl, G. R., Holmes, A., Ren-Patterson, R., Hall, F. S., Sora, I., Detera-Wadleigh, S., and Lesch, K. P. (2003) *Genes Brain Behav.* **2,** 350–364
5. Zohar, J., Chopra, M., Sasson, Y., Amiaz, R., and Amital, D. (2000) *World J. Biol. Psychiatry* **1,** 92–100
6. Tollefson, G. D. (1989) *Psychopathology* **22,** Suppl. 1**,** 37–48
7. Schatzberg, A. F. (2000) *J Clin Psychiatry* **61,** Suppl. 11**,** 9–17
8. Ricaurte, G. A., Yuan, J., and McCann, U. D. (2000) *Neuropsychobiology* **42,** 5–10
9. Rudnick, G., and Wall, S. C. (1992) *Proc. Natl. Acad. Sci. U. S. A.* **89,** 1817–1821
10. Koob, G. F. (2000) *Ann. N. Y. Acad. Sci.* **909,** 170–185
11. Zhou, F. C., Xu, Y., Bledsoe, S., Lin, R., and Kelley, M. R. (1996) *Brain Res. Mol. Brain Res.* **43,** 267–278
12. Sur, C., Betz, H., and Schloss, P. (1996) *Eur. J. Neurosci.* **8,** 2753–2757
13. Kusumi, A., and Sako, Y. (1996) *Curr. Opin. Cell Biol.* **8,** 566–574
14. Jacobson, K., Sheets, E. D., and Simson, R. (1995) *Science* **268,** 1441–1442
15. Luna, E. J., and Hitt, A. L. (1992) *Science* **258,** 955–964
16. Hitt, A. L., and Luna, E. J. (1994) *Curr. Opin. Cell Biol.* **6,** 120–130
17. Fox, J. E. (2001) *Thromb. Haemost.* **86,** 198–213
18. Fox, J. E., Lipfert, L., Clark, E. A., Reynolds, C. C., Austin, C. D., and Brugge, J. S. (1993) *J. Biol. Chem.* **268,** 25973–25984
19. Miyamoto, E. K., Katai, K., Tatsumi, S., Sone, K., Segawa, H., Yamamoto, H., Taketani, Y., Takada, K., Morita, K., Kanayama, H., Kagawa, S., and Takeda, E. (1995) *Biochem. J.* **310**, 951–955
20. Miyamoto, S., Hadama, T., Mori, Y., Shigemitsu, O., Sako, H., and Uchida, U. (1995) *Jpn. Circ. J.* **59,** 693–703
21. Heldin, C. H. (1995) *Cell* **80,** 213–223
22. Simons, K., and Ikonen, E. (1997) *Nature* **387,** 569–572
23. Wang, J., Megha, and London, E. (2004) *Biochemistry* **43,** 1010–1018
24. Schubert, A. L., Schubert, W., Spray, D. C., and Lisanti, M. P. (2002) *Biochemistry* **41,** 5754–5764
25. Helms, J. B., and Zurzolo, C. (2004) *Traffic* **5,** 247–254
26. Scanlon, S. M., Williams, D. C., and Schloss, P. (2001) *Biochemistry* **40,** 10507–10513
27. Samuvel, D. J., Jayanthi, L. D., Bhat, N. R., and Ramamoorthy, S. (2005) *J. Neurosci.* **25,** 29–41
28. Quick, M. W. (2003) *Neuron* **40,** 537–549
29. Quick, M. W. (2002) *Int. J. Dev. Neurosci.* **20,** 219–224
30. Bauman, A. L., Apparsundaram, S., Ramamoorthy, S., Wadzinski, B. E., Vaughan, R. A., and Blakely, R. D. (2000) *J. Neurosci.* **20,** 7571–7578

31. Jess, U., El Far, O., Kirsch, J., and Betz, H. (2002) *Biochem. Biophys. Res. Commun.* **294,** 272–279
32. Carneiro, A. M., Ingram, S. L., Beaulieu, J. M., Sweeney, A., Amara, S. G., Thomas, S. M., Caron, M. G., and Torres, G. E. (2002) *J. Neurosci.* **22,** 7045–7054
33. Melikian, H. E. (2004) *Pharmacol. Ther.* **104,** 17–27
34. Blakely, R. D., Ramamoorthy, S., Schroeter, S., Qian, Y., Apparsundaram, S., Galli, A., and DeFelice, L. J. (1998) *Biol. Psychiatry* **44,** 169–178
35. Jayanthi, L. D., Samuvel, D. J., Blakely, R. D., and Ramamoorthy, S. (2005) *Mol. Pharmacol.* **67,** 2077–2087
36. Zhu, C. B., Hewlett, W. A., Feoktistov, I., Biaggioni, I., and Blakely, R. D. (2004) *Mol. Pharmacol.* **65,** 1462–1474
37. Sagot, I., Regnouf, F., Henry, J. P., and Pradel, L. A. (1997) *FEBS Lett.* **410,** 229–234
38. Lohi, O., and Lehto, V. P. (1998) *FEBS Lett.* **436,** 419–423
39. Dash, D., Aepfelbacher, M., and Siess, W. (1995) *J. Biol. Chem.* **270,** 17321–17326
40. Dash, D., Aepfelbacher, M., and Siess, W. (1995) *FEBS Lett.* **363,** 231–234
41. Rudnick, G. (1977) *J. Biol. Chem.* **252,** 2170–2174
42. Najimi, M., Maloteaux, J. M., and Hermans, E. (2002) *FEBS Lett.* **523,** 224–228
43. Nishiya, N., Iwabuchi, Y., Shibanuma, M., Cote, J. F., Tremblay, M. L., and Nose, K. (1999) *J. Biol. Chem.* **274,** 9847–9853
44. Nishiya, N., Shirai, T., Suzuki, W., and Nose, K. (2002) *J. Biochem. (Tokyo)* **132,** 279–289
45. Qian, Y., Galli, A., Ramamoorthy, S., Risso, S., DeFelice, L. J., and Blakely, R. D. (1997) *J. Neurosci.* **17,** 45–57
46. Osada, M., Ohmori, T., Yatomi, Y., Satoh, K., Hosogaya, S., and Ozaki, Y. (2001) *Biochem. J.* **355,** 691–697
47. Ramamoorthy, S., and Blakely, R. D. (1999) *Science* **285,** 763–766
48. Ramamoorthy, S., Giovanetti, E., Qian, Y., and Blakely, R. D. (1998) *J. Biol. Chem.* **273,** 2458–2466
49. Hartwig, J. H., and Kwiatkowski, D. J. (1991) *Curr. Opin. Cell Biol.* **3,** 87–97
50. Hartwig, J. H., and DeSisto, M. (1991) *J. Cell Biol.* **112,** 407–425
51. Kim-Kaneyama, J. R., Suzuki, W., Ichikawa, K., Ohki, T., Kohno, Y., Sata, M., Nose, K., and Shibanuma, M. (2005) *J. Cell Sci.* **118,** 937–949
52. Duan, S., Anderson, C. M., Stein, B. A., and Swanson, R. A. (1999) *J. Neurosci.* **19,** 10193–10200
53. Sakai, N., Kodama, N., Ohmori, S., Sasaki, K., and Saito, N. (2000) *Neurochem. Int.* **36,** 567–579
54. Mochizuki, H., Amano, T., Seki, T., Matsubayashi, H., Mitsuhata, C., Morita, K., Kitayama, S., Dohi, T., Mishima, H. K., and Sakai, N. (2005) *Neurochem. Int.* **46,** 93–105